Influence of NAO and clouds on long-term seasonal variations of surface solar radiation in Europe

Marc Chiacchio[1] and Martin Wild[1]

Received 6 April 2009; revised 1 December 2009; accepted 17 December 2009; published 18 May 2010.

[1] This study is an analysis of the seasonal all-sky surface solar radiation variability in Europe during 1970–2000 using surface observations from the Global Energy Balance Archive (GEBA). On the basis of the annual means period 1970–1985, there is a statistically significant decline of −3.0% decade^{-1} (−3.8 Wm^{-2} decade^{-1}) followed by a nonsignificant rise of 0.3% decade^{-1} (0.4 Wm^{-2} decade^{-1}) during 1985–2000. The behavior of the solar radiation for spring is similar to the annual series and has the strongest increase of 1.6% decade^{-1} (2.5 Wm^{-2} decade^{-1}) during 1985–2000. In summer a similar evolution to the annual and spring time series is shown but has a stronger decline of −3.2% decade^{-1} (−6.8 Wm^{-2} decade^{-1}) during 1970–1985. A small positive nonsignificant trend is reported for the winter means time series while a statistically significant negative trend of −2.5% decade^{-1} (−2.1 Wm^{-2} decade–^{1}) was found in autumn during 1970–2000. By comparing variations in all-sky solar radiation with changes in cloud cover and NAO, we attribute the winter and autumn trends mainly to the NAO through the modification of mid-to-low cloud cover in southern Europe and the spring and summer trends to mid-to-low cloud cover in northern Europe. However, because the cloud cover and solar radiation relationship weakens in the low-frequency variability, it suggests that other effects such as aerosols may also play a role. In addition, aerosols could be interfering with the relationship between solar radiation and NAO, contributing to a strengthening of their correlation in the low-frequency variability during winter and autumn.

Citation: Chiacchio, M., and M. Wild (2010), Influence of NAO and clouds on long-term seasonal variations of surface solar radiation in Europe, *J. Geophys. Res.*, *115*, D00D22, doi:10.1029/2009JD012182.

1. Introduction

[2] The downward surface shortwave radiation is an important parameter for studying the Earth's climate system and is one of the key components of the surface energy budget. Thus, it is essential to study its spatial and temporal distribution. Studies have been done to determine its changes involving surface observations [*Ohmura and Lang*, 1989; *Liepert and Kukla*, 1997; *Gilgen et al.*, 1998; *Philipona et al.*, 2004; *Wild et al.*, 2005; *Dutton et al.*, 2006; *Behrens*, 2007], by simulating the surface radiative fluxes in General Circulation Models [*Wild et al.*, 1997; *Romanou et al.*, 2007; *Wild*, 2009a] and from a satellite perspective [*Stackhouse et al.*, 2000; *Chiacchio et al.*, 2004; *Pinker et al.*, 2005; *Petrenz et al.*, 2007] by applying radiative-transfer algorithms. Using surface observations that span from 1960 to the present time have enabled a longer-term study of this radiative parameter. From the above mentioned references, a widespread decrease of the downward solar radiation up until about 1990 has been reported and is referred as global dimming [*Gilgen et al.*, 1998; *Stanhill and Cohen*, 2001; *Liepert*, 2002]. Also, after the early 1990s an increase in the trends (brightening) is observed in many locations such as Europe and North America [*Wild et al.*, 2005; *Pinker et al.*, 2005; *Ruckstuhl et al.*, 2008; *Long et al.*, 2009].

[3] Surface observations from the Global Energy Balance Archive (GEBA) are used in this paper to study the annual and seasonal mean changes in the downward surface shortwave radiation (DSW hereinafter representing the all-sky surface downward solar radiation) on a decadal and interannual timescale. Using an earlier version of this data set, *Gilgen et al.* [1998] found a 2% decade^{-1} decrease in DSW from most sites that were available between 1965 and 1990 in Europe, North America, Asia, and Africa. In addition, *Liepert* [2002] also used data from GEBA as well as from the National Solar Radiation Database and found a 4% or 7 Wm^{-2} decrease in worldwide locations and a 10% or 19 Wm^{-2} decrease from stations within the United States from 1961 to 1990. Moreover, from the GEBA being periodically updated, this data set is reanalyzed [*Gilgen et al.*, 2009] to determine new results globally using longer time series. The time series span from 1960 to 2000 and take advantage of the longer time period as compared to the satellite period of the DSW. The

[1]Institute for Atmospheric and Climate Science, ETH Zurich, Zurich, Switzerland.

0148-0227/10/2009JD012182

results show a decrease up until the 1980s, which is followed by a subsequent increase and was noted in such regions as Europe, China, Japan, some sites in North America, the South Pole and American Samoa.

[4] Though the causes for these decadal variations in the DSW are still not clear, it has been proposed that changes in the anthropogenic aerosols may be the major cause of the global dimming phenomena [*Stanhill and Cohen*, 2001; *Liepert and Tegen*, 2002]. Particulates such as anthropogenic aerosols affect the way radiation is transmitted in the atmosphere; they play an important role in the climate system and act as a modulator of solar radiation and pose one of the largest uncertainties in climate change studies. Thus, the knowledge of their properties, temporal and spatial distribution, and interaction with solar radiation on a global level play an important role to explain many of the anthropogenic changes in the climate [*Tegen et al.*, 2000]. Aerosols can influence solar radiation directly by scattering (sulfate particles), which is called the direct effect [*Ångström*, 1962; *Schulz et al.*, 2006; *Marmer et al.*, 2007] or indirectly (indirect aerosol effect), in which they change the number of cloud condensation nuclei particles that also changes the albedo [*Twomey et al.*, 1984] and lifetime of clouds [*Lohmann and Feichter*, 2005]. The direct and indirect aerosol effects may be the main explanation for both the dimming and brightening [*Wild et al.*, 2005]. In fact, consistent regional as well as global patterns have been found between changes of solar radiation and aerosols, in particular the annual trends of sulfur and black carbon emissions during the period from 1980 to 2000 [*Streets et al.*, 2006]. A similar study was made to determine the influence of aerosols on solar radiation by *Norris and Wild* [2007] where the dimming and brightening periods were evaluated. By separating cloud cover effects from the solar radiation at European stations, the dimming and brightening was still observed and with much less noise attributing the changes to aerosol effects.

[5] Another contribution that has been proposed to these changes in the DSW is from variations in cloud cover [*Dutton et al.*, 2004, 2006]. Cloud cover variability greatly affects the incoming solar radiation even on longer timescales. In the work of *Sanchez-Lorenzo et al.* [2008], where trends of sunshine duration measurements in Europe were computed on a seasonal basis, they found that during a particular season such as in winter, changes in the circulation patterns alter cloud cover, which greatly affects the DSW. This is also consistent with the study by *Stjern et al.* [2009] where they investigate the changes in DSW using stations in northern Europe. For some stations that were analyzed on an annual basis, the changes in the concentrations of the aerosols were given as the main cause of the radiation changes. However, when they looked at the monthly trends it revealed an alternative explanation; the cloud cover changes explained the variations in the DSW. Also, depending on the location of the stations, the trends in the DSW were either explained by changes in aerosols, cloud cover, or a combination of both. However, these studies have not taken into account the low-frequency variability of cloud cover, which would indicate if the changes in cloud cover are persistent in governing the long-term variations in DSW. In this study we perform this type of analysis to explain the overall contribution of total cloud cover to changes in DSW in different seasons. In addition, the correlation between cloud cover, according to 9 different cloud types, and measurements of DSW will be determined. The question though still remains unanswered as to how much these cloud effects are associated with the influence of other factors such as the changes in aerosols [*Trenberth et al.*, 2007, p. 279].

[6] Because few studies so far have focused on the seasonal decadal variations in surface solar radiation measurements in Europe, our main objective is to determine and explain the causes of the seasonal trends from the interannual and decadal variability of the DSW in Europe during 1970–2000. We will evaluate where and in what seasons the strongest decrease/increase are occurring. Also, the impact of any relevant atmospheric circulation pattern on the DSW, such as the North Atlantic Oscillation (NAO), will also be determined. It will be known whether the cloud cover and NAO relationships with the DSW persist even when the low-frequency variability is computed for the time series, which gives an indication for their overall contribution to the decadal changes in DSW. This study can also serve as a reference for different climate model and satellite evaluations over Europe. As a follow up study a further exploration will be made on the relative importance of other influencing factors, such as aerosols on a seasonal basis in the clear-sky DSW.

2. Data and Methodology

2.1. Solar Radiation Measurements

[7] The GEBA database comprises over 2000 globally distributed stations and presently includes about 450,000 quality-controlled monthly mean values of various surface energy parameters, such as global, direct, diffuse, and other related energy components. The database was established as early as 1985 at the Swiss Federal Institute of Technology (ETH) in Zurich, Switzerland and data sources for this database include those from the World Radiation Data Center in St. Petersburg, national weather services, and other various institutions that maintain their own pyranometer stations. This data set was first implemented in 1988 [*Ohmura et al.*, 1989] and was made available to the scientific community in 1991. It was first updated in 1994 and 1995 and was made available to the Internet in 1997 [*Ohmura et al.*, 1997]. The main uses of this data set have been to study the surface energy balance, validate satellite radiation algorithms, validate energy fluxes simulated from general circulations models, and to provide data for industrial applications.

[8] There are different instruments that measure the energy parameters contained in the GEBA database. Thus, in this data set are the station histories that include the changes in the instrumentation as well as quality assessment procedures that flag the data when they are suspected to contain errors. The accuracy of the energy fluxes and the determination of the error flags depend on the type and the maintenance of the instrument as well as the data acquisition method. In addition, it becomes important to identify the number and lengths of periods of measurements that were taken in extreme weather conditions or when instruments failed and the care used for the evaluation and processing of the observations. Five quality control procedures were applied to the data, which is also important for evaluating their accuracy and to eliminate gross errors that would greatly affect the climatological means [*Gilgen and Ohmura*, 1999].

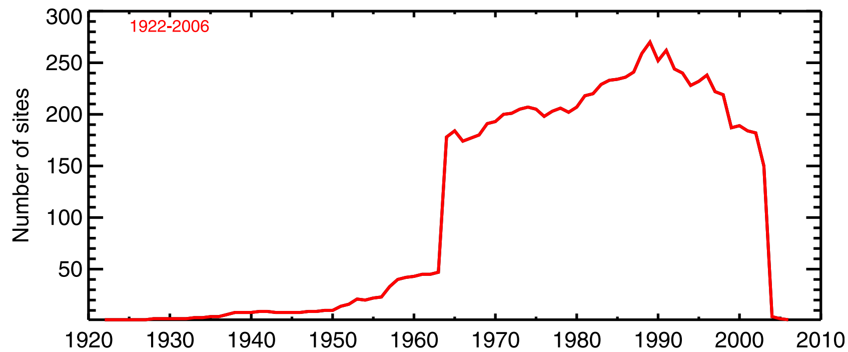

Figure 1. Temporal evolution of the number of Global Energy Balance Archive (GEBA) stations in Europe reporting surface solar radiation measurements. The period with most sites can be determined.

In addition, from *Gilgen et al.* [1998], the random error of measurement is about 5% for the monthly mean and about 2% for the annual mean. Using a quality controlled and station history-based energy balance database such as GEBA can ensure a higher confidence in results required for climate research applications such as this one.

[9] The main focus for this work is in Europe, which includes the densest number and most reliable stations. The earliest measurement of global radiation found in the GEBA database for Europe starts in 1922 and comes from the Stockholm station. This station has the most continuous data and is followed by the stations of Wageningen since 1928 and Potsdam since 1937. Another long-term station is from Locarno-Monti that has data records that start in 1938 and is also included in this analysis. However, according to *Gilgen et al.* [2009] the data from 1955 through 1971 was discarded because it did not pass quality assessment procedures. Analysis will be taken from stations that span from 1970 to 2000 because this is the period that contains the largest number of stations (Figure 1) with the requirement that there are no more than 3 months missing within any 1 year and that there are no more than 4 years of missing data within the whole period. There are a total of 45 sites for the annual series, and 42 for the seasonal series that fulfill these criteria. The number of sites contained in the seasonal series is less than the annual because when a winter season is averaged within a year, for example, the previous year that contains a value for December could be missing. Thus, there is not a winter season for that year, but the annual average would contain a value. Also, we selected the periods 1970–1985 and 1985–2000 to correspond to the transition from dimming to brightening as suggested in earlier studies. For consistency the same number of stations are analyzed in these two time frames, which are also included within 1970–2000.

[10] In addition, the two periods are separately analyzed on their own, meaning that all sites are considered that span within that time and that they fulfill the above criteria of having no more than 3 months missing within any 1 year and no more than 4 years missing within the whole period considered. Including additional sites would give a better representation for the behavior of the changes in DSW for that particular period. For the first period, there are now 110 total sites for the annual and 108 sites for the seasonal means. In the second period, a total of 86 and 83 sites are for the annual and seasonal means, respectively.

[11] Data gaps of just a few months can introduce biases in the calculated means, therefore, care must be taken to avoid such problems. We chose a filling method using climatological values and because such low requirements were chosen for the number of missing months and years, no large biases are expected to be introduced in the averaging of the data. More details on the filled data from each station are shown in Table 1. Table 1 lists the stations used in this study, which contain continuous measurements from 1970 to 2000. Also, indicated are the number of years missing and the percentage of filled data for each site. The reason we adhered to a stricter criteria to allow only a small number of filled months is because the climate science community has become more aware that there is a need for improved handling of data that minimizes noise in order to detect a clearer signal. Moreover, this is in line with the implementation of standardized methods and calibration procedures during the last 20 years to ensure a higher quality of solar radiation measurements from various institutions [*Gilgen et al.*, 2009].

[12] Changes in the DSW from the GEBA time series (1970–2000) in Europe are detected using regression models. A technique applied to these models to select the best fit from first order to third order was accomplished by applying three steps: (1) Calculate the first-, second-, and third-order fits to the original time series; (2) calculate the correlation coefficient from the fits and time series; and (3) calculate the residuals of the three fits from the original data and their standard error. The best fit from these time series is then selected according to the highest values to their corresponding correlations and the lowest values of their standard error. To calculate the trends from the divided periods, 1970–1985 and 1985–2000, a first-order fit is determined for the line as well as confidence intervals using the bootstrap method. This method takes into account the standard error of the best fit line as well as the uncertainty of the measurement error to quantify their contributions to the total uncertainty. In addition, the autocorrelation is used to detect randomness in the data at varying time lags. The time series is considered random when the autocorrelations of the residuals are within the 95% confidence limits or within $\pm(2/N^{1/2})$, where N is the number of data points in the time series. If the autocorrelation test does show randomness in the data, then it gives assurance that the linear regression model used is appropriate and valid. This test was applied to all the time series analyzed, which were

Table 1. Details of the Long-Term GEBA Sites Used in This Study[a]

Site	Country	Lat	Lon	Missing (year)	Filled (%)
Aberporth	GB	52.10	−4.57	1	3.5
Ajaccio	FR	41.90	8.80	3	1.3
Aldergrove-Airprt.	GB	54.60	−6.22	2	0.8
Amendola	IT	41.50	15.71	0	2.2
Belsk	PL	51.80	20.78	0	0.0
Bergen	NO	60.40	5.31	0	1.1
Bracknell	GB	51.30	−0.79	1	0.8
Bratislava	SK	48.10	17.10	4	0.3
Braunschweig	DE	52.30	10.45	0	1.3
Budapest	HU	47.40	19.18	2	1.3
De Bilt	NL	52.10	5.18	0	0.8
Eskdalemuir	GB	55.30	−3.20	1	1.9
Hamburg	DE	53.60	10.11	0	1.6
Hradec Kralove	CZ	50.20	15.85	0	0.5
Jokioinen	FI	60.80	23.50	0	0.5
Kilkenny	IE	52.60	−7.27	1	2.7
Kiruna	SE	67.80	20.23	1	5.1
Klagenfurt	AT	46.60	14.33	3	2.4
Kolobrzeg	PL	54.10	15.58	0	0.0
Lerwick	GB	60.10	−1.19	0	2.2
Limoges	FR	45.80	1.28	2	0.5
Locarno-Monti	CH	46.10	8.78	0	0.3
London Weather C.	GB	51.50	−0.12	2	2.2
Lulea	SE	65.50	22.13	0	2.7
Millau	FR	44.10	3.01	1	1.1
Nancy-Essey	FR	48.60	6.21	2	0.8
Nice	FR	43.60	7.20	2	1.1
Odessa	UA	46.40	30.63	2	0.5
Reykjavik	IS	64.10	−21.90	1	5.4
Sljeme/Puntijarka	HR	45.90	15.96	1	1.1
Sodankyla	FI	67.30	26.65	0	8.6
Sonnblick	AT	47.00	12.95	4	1.3
St.Hubert	BE	50.00	5.40	3	2.2
Stockholm	SE	59.30	17.95	0	1.3
Taastrup/Copenhagen	DK	55.60	12.30	0	1.3
Trier	DE	49.70	6.66	0	0.0
Uccle	BE	50.80	4.35	0	0.5
Valentia	IE	51.90	−10.25	1	0.0
Vigna di Valle	IT	42.00	12.21	1	3.0
Wageningen	NL	51.90	5.65	0	0.5
Warszawa	PL	52.20	20.98	0	0.0
Weihenstephan	DE	48.40	11.70	1	1.6
Wien-Hohe-Warte	AT	48.20	16.36	3	0.0
Wuerzburg	DE	49.70	9.96	0	0.5
Zakopane	PL	49.20	19.96	0	0.5

[a]Each site listed contains surface solar radiation measurements that are continuous and cover the period from 1970 to 2000. The number of years missing for each site is indicated along with the percentage of filled data. Sites underlined denote those that are not included in the seasonal means. GEBA, Global Energy Balance Archive. Country codes are as follows: AT, Austria; BE, Belgium; CH, Switzerland; CZ, Czech Republic; DE, Germany; FI, Finland; FR, France; GB, United Kingdom; HR, Croatia; HU, Hungary; IE, Ireland; IS, Iceland; IT, Italy; NL, Netherlands; NO, Norway; PL, Poland; SE, Sweden; SK, Slovakia; UA, Ukraine.

found to be random within the 95% confidence limit. Thus, the statistical model used to compute the best fit line is accurate. This model is of the form, $Y = \alpha + \beta X + N$, where α is the y intercept, β is the slope or trend of the line, X is the time variable, and N is the error. To apply the bootstrap method to this linear model we use the approach of resampling the residuals. First we choose an initial value to simulate from, such as the 2% measurement uncertainty for the annual mean [*Gilgen and Ohmura*, 1999]. For a seasonal mean uncertainty measurement we choose 3%, which is slightly larger than the annual mean but smaller than the monthly mean uncertainty of 5%. A random error distribution is produced from this estimated measurement uncertainty and is added to the original measurement values to compute a best fit line. The trend (β_i) is then computed from this line and its standard error (σ_i), which is repeated many times. From these simulated trends, the mean (β_{mean}) is taken and is used as the true trend. To compute the confidence intervals, the bootstrap variance is first needed using the formula: Variance(β) = $1/m\ \Sigma(\sigma_i)^2$ + Variance(β_i), where m is the number of simulations and is set to 1000. This formula represents the mean of all the stored bootstrap estimates of the standard error of the fit squared plus the variance of the simulated trends. The first term is caused by the standard errors of the individual fits and the second term is caused by the uncertainty of the measurement error. To calculate the upper and lower limits of the confidence interval at the 5% significance level we use $\pm t\,(\text{Variance}(\beta))^{1/2}$, where t is the t statistic with $p = 0.05$.

2.2. North Atlantic Oscillation Index

[13] The monthly NAO index used to compute the correlation with the DSW for the seasonal mean series is obtained from Jim Hurrell from the Global and Climate Dynamics Division (CGD) Climate Analysis Section at the National Center for the National Center for Atmospheric Research (NCAR) in Boulder, Colorado in the United States. This index represents the difference in normalized sea level pressure (SLP) between Ponta Delgada, Azores and Stykkisholmur/Reykjavik, Iceland. From this index we obtained the seasonal means for the whole analysis period 1970–2000. (See *Hurrell et al.* [2003] for a more detailed description of the NAO and its role in climate variability.) The correlation between the DSW and NAO is determined from the Pearson correlation coefficient at the 95% confidence level using the t value,

$$t = r\sqrt{\frac{(n-2)}{(1-r^2)}} \tag{1}$$

where r is the correlation coefficient and n is the number of data points. This t value is then compared with the critical t value with p = 0.05 by using the student's t test to see whether the null hypothesis, where no relationship exists between the two variables, is rejected. Analysis was performed for each season over different regions such as Europe, southern Europe, and northern Europe. Different time periods were chosen in order to see if better agreement results. The low-frequency variability from each time period is then computed by applying a low-pass filter, such as a simple moving average of 5 years in order to assess their long-term contribution to the changes in DSW.

2.3. Cloud Cover Observations

[14] Cloud data used is provided by the Carbon Dioxide Information Analysis Center (CDIAC), which is a data and information analysis center for the Unites States Department of Energy located at the Oak Ridge National Laboratory. This cloud data set includes annual and seasonal means of total cloud amount as well as from 9 different cloud types from 1971 to 1996. These cloud types include those from the

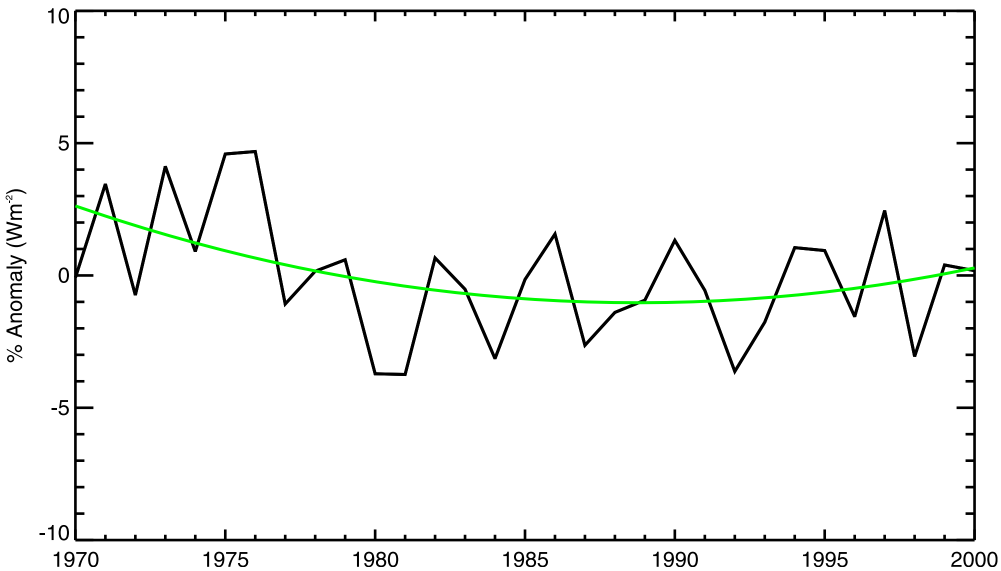

Figure 2. Annual means surface solar radiation time series between 1970 and 2000 from all GEBA sites with continuous records throughout the period studied. A second-order fit was appropriately used to determine the temporal evolution of the variations of the solar radiation.

lower level of the troposphere: cumulonimbus (CB), cumulus (CU), fog (FO), stratocumulus (SC), and stratus (ST); those from the midlevel: altocumulus (AC), altostratus (AS), nimbostratus (NS); and those from high-level clouds (HI). In the work of *Warren et al.* [2007], a cloud cover global climatology was made from this data set that included analysis from about 5400 land-based stations with over 185 million synoptic reports for the period 1971–1996. In their study they found significant regional trends of cloud cover for each cloud type. The temporal resolution of the cloud observations are every 3 h and are taken from human observers. The available data set for the land has been produced for individual stations, which is used in this study. These cloud cover sites are colocated with the GEBA sites that are within 1° latitude × 1° longitude. The actual method for computing the cloud amounts is described by *Warren and Hahn* [2002]. The data analyzed to produce these climatologies have passed through quality control and processing procedures. They also selected stations that met criteria that include a sufficient amount of observations as well as the reporting of all cloud types during the whole 26 year period.

[15] Correlation analysis is performed to determine the strength of the linear relationship between cloud cover and DSW and between cloud cover and NAO for all seasons in Europe as a whole, southern Europe, and northern Europe. The analysis between the clouds and NAO is a follow up to *Norris and Wild* [2007] where they find a strengthening of the relationship between the clouds and NAO in the low-frequency series even during summer. Here we extend this work and look at the correlation for 9 cloud types for both the high- and low-frequency variability and for different parts of Europe to detect if clouds or the NAO have a tendency to be more influential according to location, which strongly depends upon local heating and/or circulation patterns. The significance of the correlation at the 95% confidence level is determined by using equation (1) and the procedure defined above in section 2.2.

3. Analyses of Surface Solar Radiation

3.1. Annual and Seasonal Mean Changes 1970–2000

[16] Figure 2 shows the annual time series for all sites combined in this study. A second-order fit was properly applied, which clearly shows a slight decline in DSW from 1970 until around the mid-1980s. This is followed by an upward trend through the rest of the time series until 2000. Only the trend during 1970–1985 is significant (Table 2);

Table 2. Annual and Seasonal Mean Trends for the Periods 1970–1985 and 1985–2000 of Surface Solar Radiation With 95% Confidence Intervals Computed[a]

Temporal Resolution	1970–1985	1985–2000
Annual		
Percent $decade^{-1}$	**−3.0** ± 2.3	0.3 ± 1.7
Wm^{-2} $decade^{-1}$	**−3.8** ± 3.5	0.4 ± 2.9
Winter (DJF)		
Percent $decade^{-1}$	0.5 ± 1.5	Monotonic time series
Wm^{-2} $decade^{-1}$	0.2 ± 0.7	Monotonic time series
Spring (MAM)		
Percent $decade^{-1}$	−2.4 ± 3.5	1.6 ± 2.9
Wm^{-2} $decade^{-1}$	−3.7 ± 6.5	2.5 ± 5.9
Summer (JJA)		
Percent $decade^{-1}$	−3.2 ± 3.8	0.9 ± 2.3
Wm^{-2} $decade^{-1}$	−6.8 ± 9.4	1.9 ± 6.8
Autumn (SON)		
Percent $decade^{-1}$	**−2.5** ± 1.5	Monotonic time series
Wm^{-2} $decade^{-1}$	**−2.1** ± 1.4	Monotonic time series

[a]Monotonic time series have only one trend computed for 1970–2000. Bold values denote statistical significance. DJF, December-January-February; MAM, March-April-May; JJA, June-July-August; SON, September-October-November.

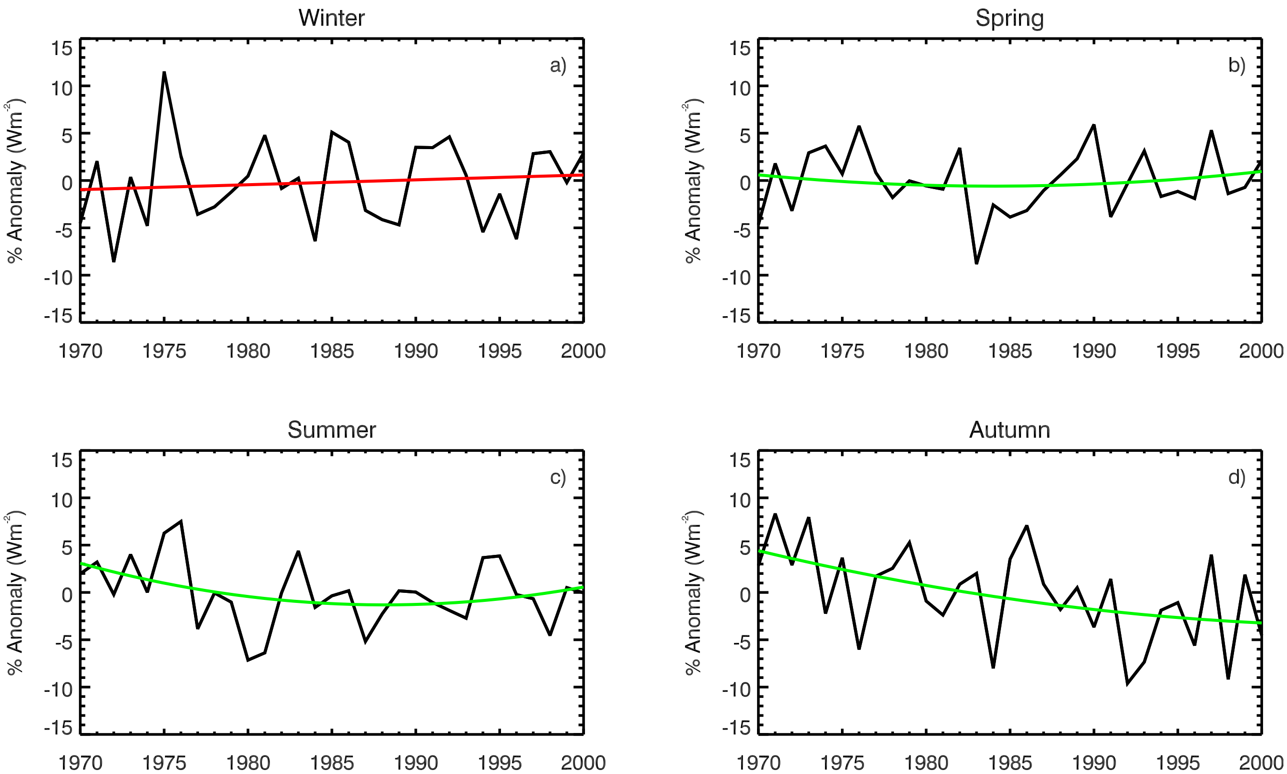

Figure 3. Seasonal means surface solar radiation time series between 1970 and 2000 from all GEBA sites studied: (a) winter (December-January-February (DJF)); (b) spring (March-April-May (MAM)); (c) summer (June-July-August (JJA)); and (d) autumn (September-October-November (SON)). Fits from first to third order were appropriately applied to determine the temporal evolution of the variations of the solar radiation.

however, these trends overall agree with those given by *Norris and Wild* [2007] where they report a decrease followed by an increase since the mid-1980s or in the 1990s in Europe.

[17] The winter mean time series is shown in Figure 3a, and a first-order fit has been determined as most appropriate to detect any changes over the whole period. The trend is close to zero with an indication for a slight overall increase; however, it is nonsignificant at the 95% confidence level, which implies that it cannot be distinguished from a trend that is zero. The behavior of the DSW for spring (Figure 3b) is similar to the annual series with a minimum reached in 1983 and has the strongest increases during the later part of the period from all the series shown. In summer (Figure 3c) the changes in DSW show a similar evolution to the annual and spring time series. Also, the decrease found during the early part of the period is slightly stronger when compared to the spring series. A maximum value is reached in 1976 with a series of minimum values from 1977 to 1981. Both spring and summer trends are, however, not significant. In Figure 3d, the autumn series shows a strong downward trend throughout the whole period and is significant.

3.2. Annual and Seasonal Mean Changes 1970–1985

[18] The annual mean changes from each individual station's time series is shown in Figure 4. It shows overall that the trends throughout Europe are negative with values declining below −12% decade^{-1} (−12 Wm^{-2} decade^{-1}) and only about one third of them are significant. Large negative values are found in the northern part of Europe with a maximum decrease of −13.3% decade^{-1} (−12.4 Wm^{-2} decade^{-1}) in Sodankyla, Finland. When all available sites are included for this period regardless of their consistency to the other period, negative trends still prevail for a large majority of the sites (figure not shown). There are also large decreases in the Mediterranean region and about half of them are statistically significant. Stations with nonsignificant trends are mainly confined to central Europe. Table 2 shows the annual mean trends from the average of all sites for the two time periods shown in Figure 2. After applying first-order linear fits to the annual mean series for 1970–1985, a statistically significant decrease of −3.0% decade^{-1} (−3.8 Wm^{-2} decade^{-1}) is detected.

[19] In the seasonal mean time series for winter (Figure 5a) sites located primarily in central and northern Europe have positive trends for the period 1970–1985. From these sites only seven are significant. The maximum increase is 19.7% decade^{-1} in Lulea, Sweden. Stations in the Mediterranean show negative trends with a majority of them being nonsignificant. If stations are added that cover only this time period, a greater number of sites display large positive values mainly in the central part of Europe (figure not shown). In spring (Figure 5b) most sites have negative trends and are nonsignificant, which is similar to the annual series. If we compare Figure 5b to the results that have additional sites included for this period, more sites are included that have significant

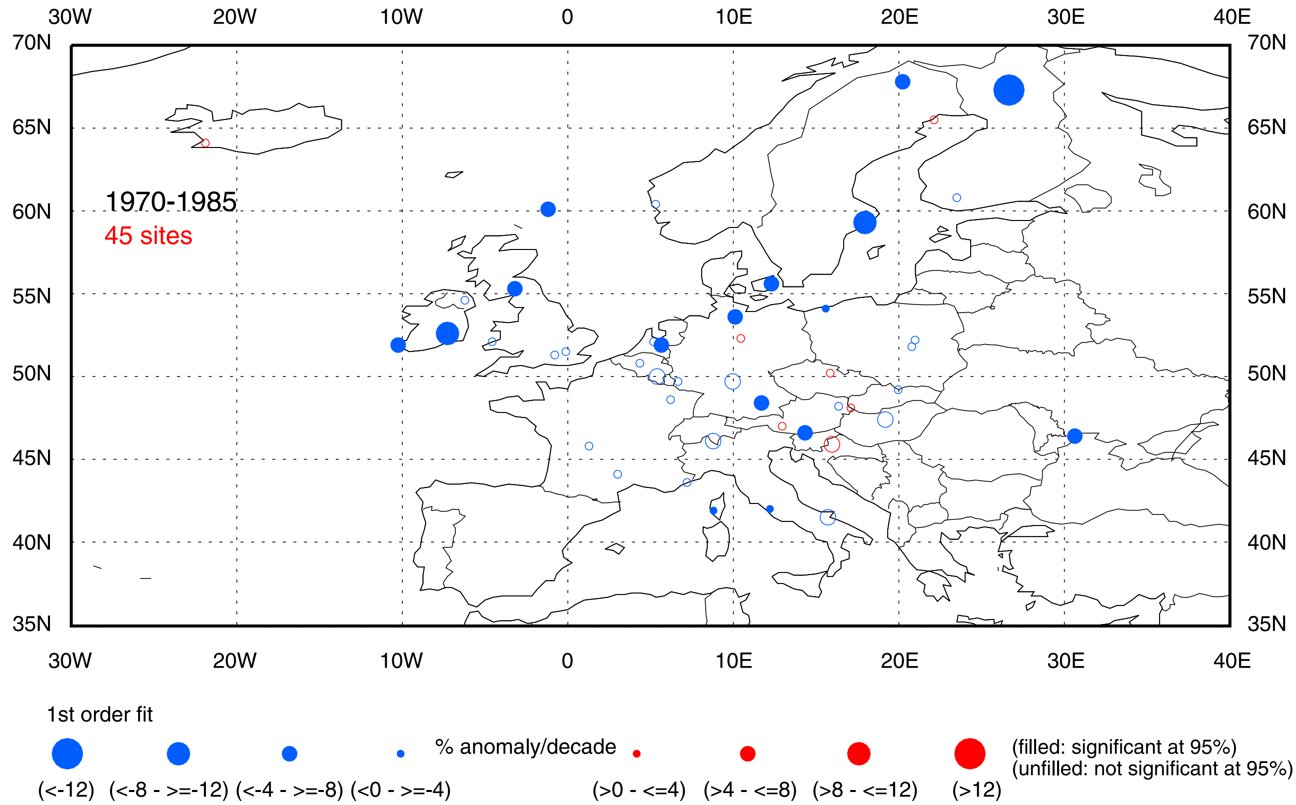

Figure 4. Magnitudes and their signs of trends (red circles for increases and blue circles for decreases) computed from annually averaged surface solar radiation in % decade^{-1} for the period 1970–1985. Significant trends at the 95% confidence level are filled circles, and nonsignificant trends are unfilled circles.

negative trends in the Mediterranean. We find similar results for the summer season (Figure 5c) but with larger decreases in northern Europe. By including the additional sites, large negative trends (significant) are also found in the Mediterranean region. Finally, the overall behavior in the autumn season is a decrease with large and significant values found mainly in the United Kingdom (Figure 5d). If we include the additional sites, southern Europe also shows negative trends and about half of them are significant.

[20] The trends per decade for the different seasons are shown in Table 2 from the average of all stations considered and thus, the overall changes in DSW can be evaluated. In winter there is a slight increase in DSW of 0.5% decade^{-1} (0.2 Wm^{-2} decade^{-1}) throughout the whole period from 1970 to 2000. The spring, however, during 1970–1985 shows a large decrease of −2.4% decade^{-1} (−3.7 Wm^{-2} decade^{-1}). A higher value of linear change is found in the summer with a decrease of −3.2% decade^{-1} (−6.8 Wm^{-2} decade^{-1}). Finally, in autumn the trend is −2.5% decade^{-1} (−2.1 Wm^{-2} decade^{-1}) throughout the period 1970–2000. The only seasonal mean trend for this period that is statistically significant is autumn.

3.3. Annual and Seasonal Mean Changes 1985–2000

[21] The trends for the annual means from 1985 to 2000 show an increase or brightening for 36 out of 45 sites. Only eight stations located in eastern and southern Europe are significant but show the largest increase of 4–8% decade^{-1} (4–8 Wm^{-2} decade^{-1}) (Figure 6). The linear changes in DSW computed for this period from the average of all sites, show a positive trend of 0.3% decade^{-1} (0.4 Wm^{-2} decade^{-1}) but is not significant (Table 2).

[22] In winter for this period, a dipole pattern has developed between negative values in the central and northern part of Europe and positive values in the south (Figure 7a). If we confine sites only to this period, it strengthens the pattern seen above (figure not shown). There are now additional sites that show positive trends in the south and three of them are significant. The spring is similar to the trends for the annual means. Most sites have positive values, which include eight sites that are statistically significant in eastern and southern Europe (Figure 7b). In summer the sites mirror the behavior of the spring time series (Figure 7c). In autumn a different and opposite pattern from winter emerges with positive trends now located in the north with values larger than 8% decade^{-1} (8 Wm^{-2} decade^{-1}) and negative trends less than −12% decade^{-1} (−12 Wm^{-2} decade^{-1}) in the south (Figure 7d).

[23] The trends for the seasonal mean time series for 1985–2000 are shown in Table 2, however, they are not statistically significant. In spring an increase by as much as 1.6% decade^{-1} (2.5 Wm^{-2} decade^{-1}) is computed. This season has the largest increase in DSW during 1985–2000 among the annual and all other seasons. In summer the increase in DSW during this period is not as strong, but still has a value of 0.9% decade^{-1} (1.9 Wm^{-2} decade^{-1}).

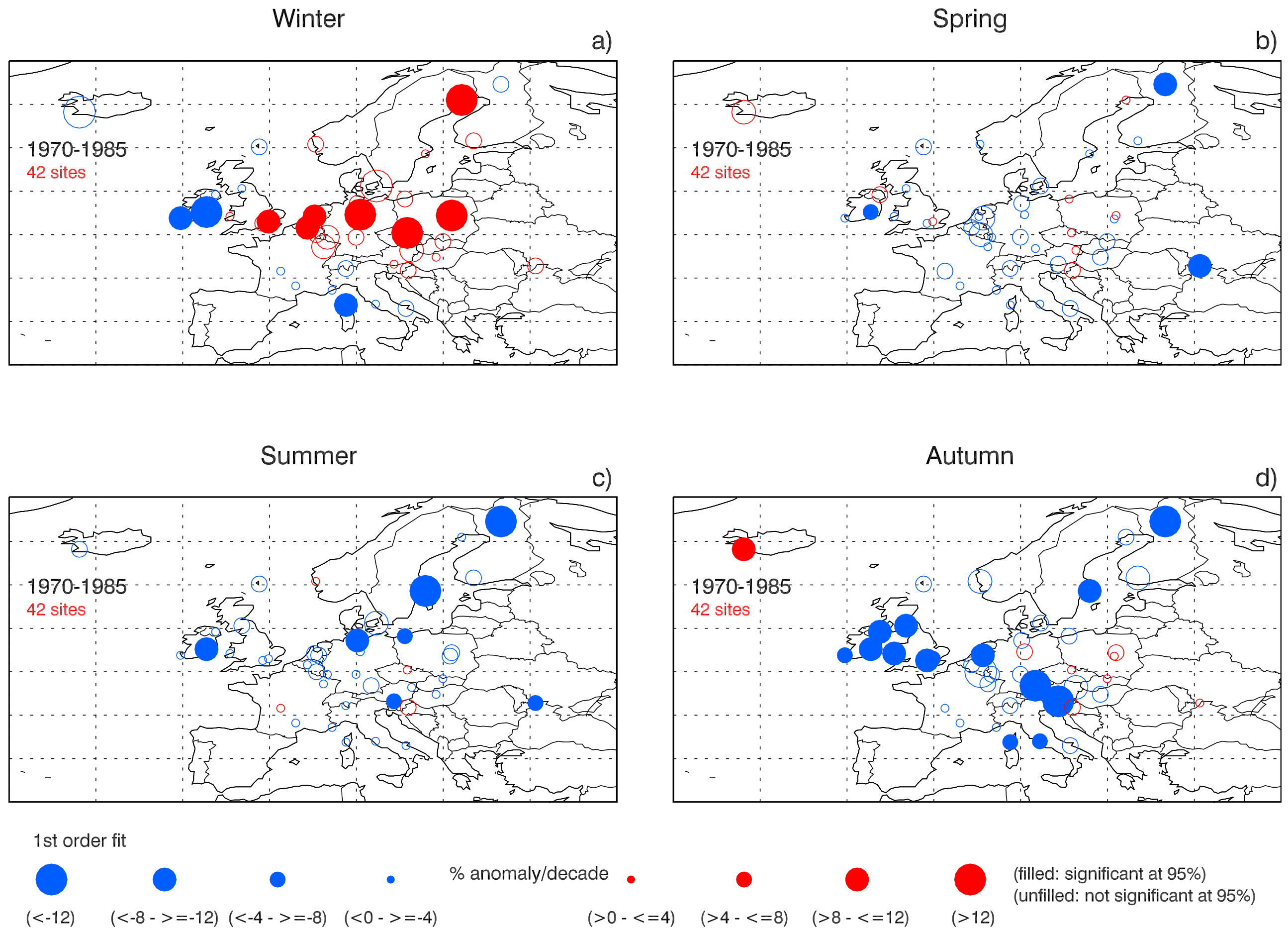

Figure 5. As in Figure 4 but for seasonal means surface solar radiation: (a) winter (DJF); (b) spring (MAM); (c) summer (JJA); and (d) autumn (SON).

3.4. Influence From the North Atlantic Oscillation

[24] Table 3 shows the correlation coefficients for the DSW and NAO index in each season and for three periods studied for all of Europe, southern Europe, and northern Europe. Southern Europe displays the highest correlation out of the three regions primarily in winter. In southern Europe for the period 1970–2000, the correlation is 0.68 and is statistically significant. In the low-frequency time series, the correlation improves to a value of 0.82, which is also significant. Figure 8 shows the temporal evolution of the DSW together with the NAO index for winter during 1970–2000 for southern Europe. The smoothed series is also seen in Figure 8 to show the low-frequency variations and the persistence of the close relationship between the two variables. Moreover, Figure 9 shows a more detailed analysis of the correlation coefficients for each site analyzed for the same period and season. It reveals a dipole pattern with negative correlations in the north and positive correlations in the south.

[25] By subdividing the period 1970–2000, as applied in the trend analysis of the DSW, the relative strength of the NAO influence on the DSW can be determined. For example, if we confine the correlation to 1970–1985, lower values are reported in winter and are also nonsignificant. When the period 1985–2000 is taken, a good statistically significant correlation of 0.74 is found in southern Europe in winter. The low-frequency variability reveals an even higher and significant correlation of 0.95. Overall the correlation increases in winter from the high- to low-frequency series. What is also noticeable for the low-frequency series is the fairly good agreement in autumn of 0.58 and 0.47 in southern Europe for the periods 1970–2000 and 1985–2000, respectively. In northern Europe fair negatively correlated values in winter of −0.52 for 1970–2000 and −0.59 for 1985–2000 are shown in the low-frequency variability.

[26] Table 4 is the seasonal relationship between total cloud cover and NAO index during 1971–1996 for 9 different cloud types for all of Europe, southern Europe, and northern Europe. As shown in the DSW and NAO relationship, the correlation for the cloud cover displays an increase when the low frequency is computed for the time series. This also applies for most cloud types in some seasons. Highest values are displayed in southern Europe in winter with a correlation of −0.79 and −0.90 for the low-frequency variability and both are statistically significant. For all of Europe in winter a high value of −0.76 is obtained for the low-frequency variability. Note also the good correlation in Europe and northern Europe for the total cloud, low-frequency series in spring and summer, which are all significant. Overall the correlation between cloud cover and NAO is stronger than between DSW and the NAO.

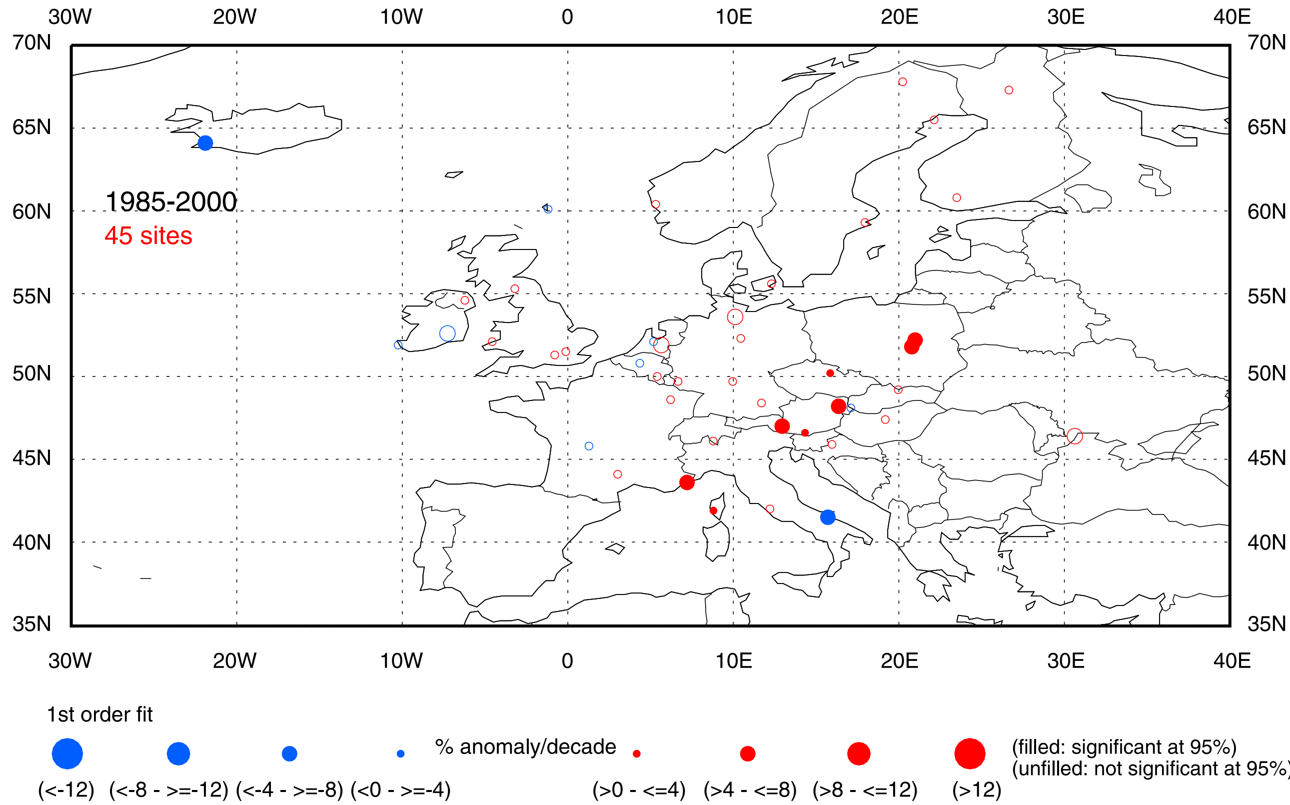

Figure 6. Magnitudes and their signs of trends (red circles for increases and blue circles for decreases) computed from annually averaged surface solar radiation in % decade^{-1} for the period 1985–2000. Significant trends at the 95% confidence level are filled circles, and nonsignificant trends are unfilled circles.

[27] The cloud types that show the strongest correlation between cloud cover and NAO for all of Europe are altostratus, fog, high, nimbostratus, stratocumulus, and stratus. Maximum values are found in altostratus with −0.66 and −0.75 in winter, which are both significant. For this cloud type in southern Europe during winter, correlations are lower with values of −0.52 and −0.62 but are significant. In southern Europe best agreement between cloud cover and NAO is seen in nimbostratus with values of −0.71 and −0.77 and both are significant.

3.5. Relationship Between DSW and Cloud Cover

[28] The relationship between the DSW and cloud cover was also analyzed with results reported in Table 5. It shows the seasonal correlation coefficients for all 9 cloud types and three regions during 1971–1996. What is evident, unlike the DSW and NAO or the cloud cover and NAO, is the decrease in correlation after the time series is smoothed using the 5 year running average. Figure 10 shows the seasonal means time series for all of Europe for the DSW and the opposite of total cloud amount in all of Europe. The correlation in all seasons computed for the period 1971–1996 are almost all significant but decrease in the low-frequency series. In general, this applies to most cloud types in all seasons. The total cloud cover correlation with DSW has a maximum value in summer in northern Europe of −0.93 and is statistically significant, but decreases to −0.81 in the low-frequency series. Overall the best agreement for total cloud cover is seen in Europe and northern Europe for spring and summer and in southern Europe for winter and autumn. Cloud types that show the strongest correlation with the DSW are the nimbostratus, stratocumulus, and stratus clouds, which are mid-to-low-level clouds. Out of these three cloud types, maximum values are shown in the nimbostratus clouds.

4. Discussion

[29] The analyses of our annual mean time series for all of Europe show reductions in the DSW during the 1970s and 1980s and is in agreement with many studies carried out in Europe and other parts of the world [*Russak*, 1990; *Stanhill and Kalma*, 1995; *Abakumova et al.*, 1996; *Liepert and Kukla*, 1997; *Gilgen et al.*, 1998; *Stanhill and Cohen*, 2001; *Liepert*, 2002; *Power*, 2003; *Alpert et al.*, 2005; *Dutton et al.*, 2006; *Ohmura*, 2006; *Gilgen et al.*, 2009; *Wild*, 2009b]. After the mid-1980s the trends in the DSW show a reversal during the mid-1980s and is referred to as brightening [*Wild et al.*, 2005; *Pinker et al.*, 2005; *Gilgen et al.*, 2009; *Ruckstuhl et al.*, 2008; *Long et al.*, 2009]. In particular, the annual mean trends overall agree with those found by *Norris and Wild* [2007]. What is not consistent with this study are the trends detected for winter and autumn, which are most likely due to the different definitions of the seasons. The results shown from our study are also in line with the decadal changes of diurnal temperature range measurements from *Makowski et al.* [2009] and sunshine duration from *Sanchez-Lorenzo et al.* [2008].

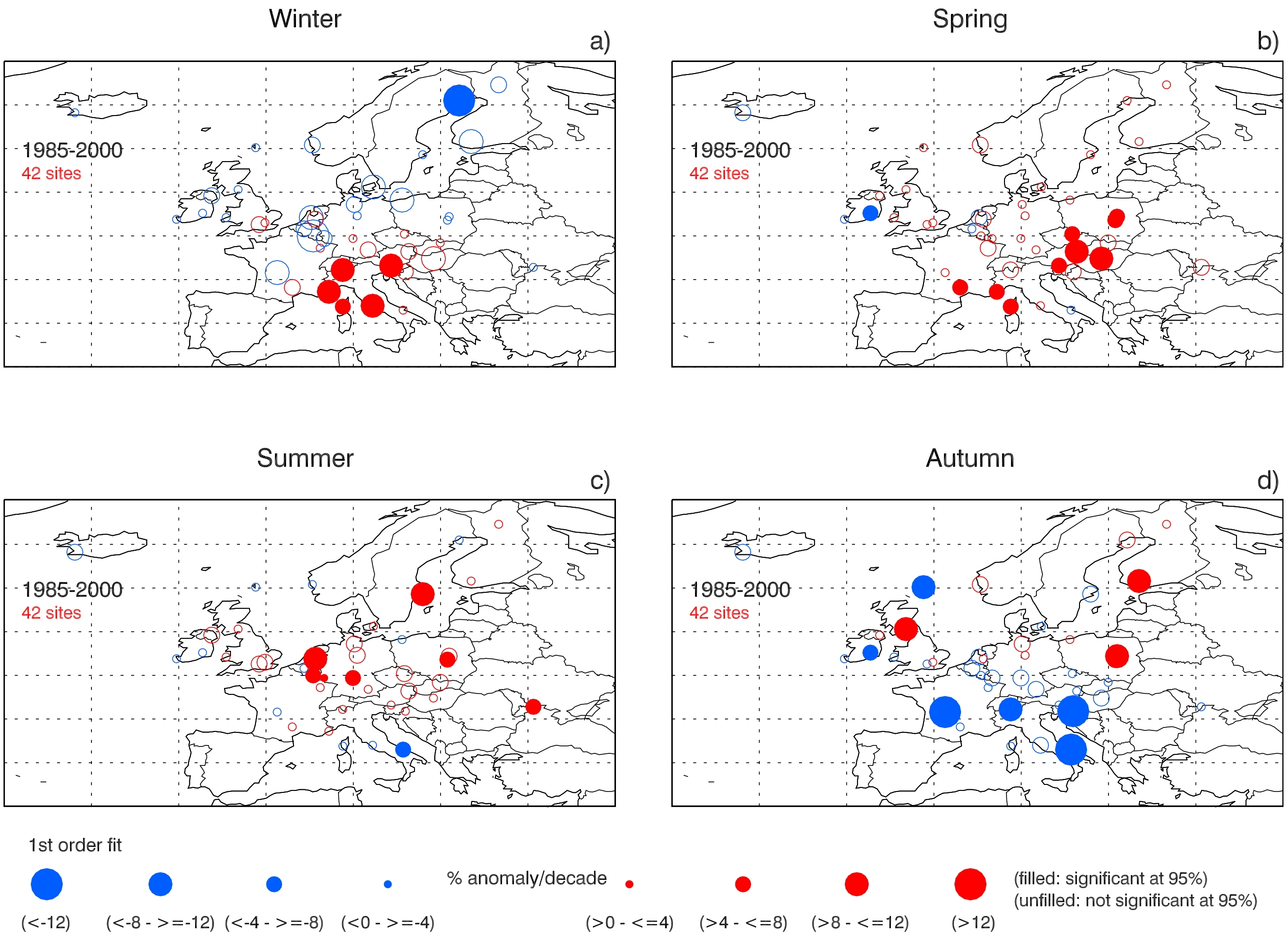

Figure 7. As in Figure 6 but for seasonal mean time series: (a) winter (DJF); (b) spring (MAM); (c) summer (JJA); and (d) autumn (SON).

[30] It seems logical that the potential causes for the annual mean evolution of these trends for all of Europe during 1970–2000 are generally related to the changes in the transmissivity of the atmosphere or modifications to the aerosol loadings in Europe over this period [*Norris and Wild*, 2007]. Moreover, the peak emissions of these aerosols, such as sulfur dioxide, occur in Europe in the 1980s [*Mylona*, 1996; *Marmer et al.*, 2007; *Vestreng et al.*, 2007]. This change in the aerosols occurs about the same time that the reversal is seen in the annual mean temporal evolution of the DSW.

[31] In particular, sulfur dioxide emissions in Europe have been reduced in the last 20 years from enforced air pollution regulations [*Streets et al.*, 2006] as well as the breakdown of the economy in the former Soviet Union. From 1980 to 1989 there has been a 20% reduction of sulfur emission in western Europe and a 54% reduction in central and eastern Europe during 1990–1999 [*Vestreng et al.*, 2007]. Also, there has been a reduction in aerosol optical depths of up to 60% from a number of sites in northern Germany and Switzerland [*Ruckstuhl et al.*, 2008]. The negative trends from our results of the DSW during 1970–1985 for eastern Europe is in agreement with the large increase in emissions of aerosols at this time. Also, negative trends still persist in western Europe during this period. During 1985–2000 the

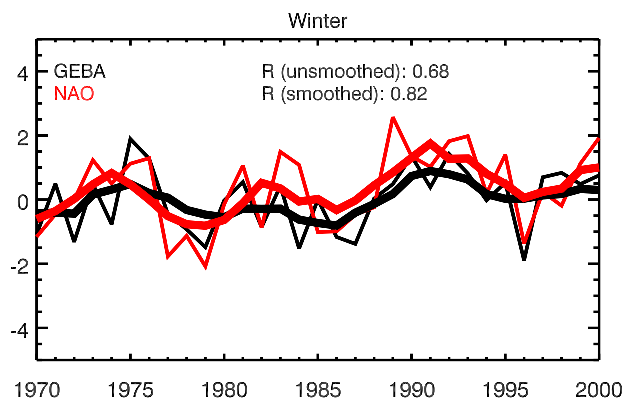

Figure 8. Winter (DJF) means time series of surface solar radiation in black and the North Atlantic Oscillation (NAO) winter index in red for southern Europe for the period 1970–2000. The correlation coefficient is displayed both for the unsmoothed series (high-frequency variability) and for the smoothed series (low-frequency variability). The smoothed series is computed using a running average of 5 years. Units are standardized anomalies and are dimensionless.

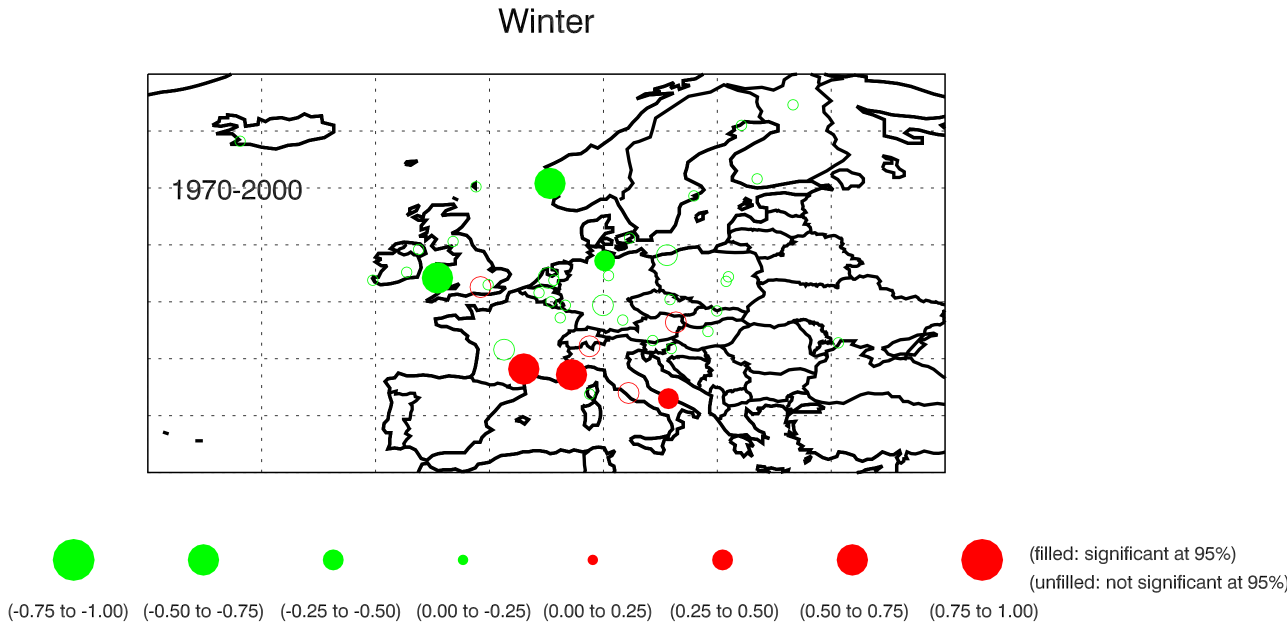

Figure 9. Map of correlation coefficients displayed for each site in winter (DJF) between the surface solar radiation and the North Atlantic Oscillation (NAO) index during 1970–2000. Magnitudes and their signs of correlation (red circles for positive and green circles for negative values) are computed. Significant correlation coefficients at the 95% confidence level are filled circles, and nonsignificant correlation coefficients are unfilled circles.

overall trend in the DSW is positive and is consistent with the reduction in aerosols over Europe during this time.

[32] Anthropogenic aerosols have been put forward as the major explanation for the annual mean changes in solar radiation; however, when the temporal evolution of the seasonal mean is considered, variations in cloud cover also seem to play a role, at least in the high-frequency variability. For winter the trend is near zero but with a slight tendency for an increase until 2000; however, because it is not significant it cannot be distinguished from a trend that is zero. If we look at the map of trends for the individual stations during 1970–1985, the winter shows a remarkable feature that is not evident in the seasonal means time series aggregated from the sites (see Figures 3a and 5a). It shows that sites mostly located in the eastern and central parts of Europe have positive and significant trends that are greater than 12% decade^{-1}. From the correlation analysis, this period shows a weaker influence by the NAO on DSW. There is less influence by the NAO because it is primarily in its negative phase during the early part of this period to about the late 1970s [*Hurrell et al.*, 2003], which infers more storm systems in the south and an increase in anticyclonic activity in the central and northern parts of Europe [*Rodwell et al.*, 1999; *Trigo et al.*, 2002]. In addition, there was a large increase in winter pressure detected after 1970 in the central part of Europe [*Maugeri et al.*, 2004; *Sanchez-Lorenzo et al.*, 2008].

Table 3. Correlation Coefficients for Surface Solar Radiation and North Atlantic Oscillation Index[a]

	1970–2000	1970–2000 (Running Average)	1970–1985	1970–1985 (Running Average)	1985–2000	1985–2000 (Running Average)
Europe						
Winter	0.26	0.34	0.29	0.23	0.09	0.16
Spring	**0.37**	0.29	0.45	0.36	0.34	0.44
Summer	**0.62**	**0.62**	0.56	0.61	**0.75**	0.45
Autumn	0.32	**0.42**	0.07	**−0.60**	0.42	**0.57**
Southern Europe						
Winter	**0.68**	**0.82**	0.56	0.60	**0.74**	**0.95**
Spring	0.29	0.10	0.31	0.42	0.27	−0.30
Summer	−0.15	−0.07	−0.06	0.08	−0.36	−0.47
Autumn	0.30	**0.58**	0.28	−0.26	0.09	0.47
Northern Europe						
Winter	−0.34	**−0.52**	−0.11	−0.15	−0.57	−0.59
Spring	0.29	0.30	0.36	0.28	0.27	0.59
Summer	**0.66**	**0.72**	0.59	**0.65**	**0.79**	**0.66**
Autumn	0.21	0.06	0.11	**−0.66**	**0.55**	**0.63**

[a]For the entire period as well as two subperiods for each season of winter (DJF), spring (MAM), summer (JJA), and autumn (SON) for all of Europe, southern Europe, and northern Europe. A running average of 5 years is performed to assess their low-frequency variability. Bold values indicate significance at the 95% confidence level.

Table 4. Correlation Coefficients for Total Cloud Cover as Well as Cloud Cover From Nine Different Cloud Types and North Atlantic Oscillation Index[a]

Cloud Type	Europe	Europe (Running Average)	Southern Europe	Southern Europe (Running Average)	Northern Europe	Northern Europe (Running Average)
TC						
Winter	**−0.52**	**−0.76**	**−0.79**	**−0.90**	−0.09	**−0.44**
Spring	**−0.46**	**−0.75**	**−0.44**	**−0.39**	−0.34	**−0.72**
Summer	−0.08	**−0.71**	**−0.17**	**−0.23**	−0.14	**−0.75**
Autumn	**−0.25**	**−0.34**	**−0.37**	**−0.78**	−0.07	0.19
AC						
Winter	−0.27	−0.20	**−0.47**	−0.35	−0.12	−0.12
Spring	−0.22	−0.17	−0.30	−0.30	−0.10	0.03
Summer	−0.15	**−0.62**	0.17	−0.17	−0.21	**−0.65**
Autumn	−0.33	**−0.54**	−0.33	**−0.78**	−0.23	0.12
AS						
Winter	**−0.66**	**−0.75**	**−0.52**	**−0.62**	−0.35	−0.08
Spring	−0.26	−0.03	−0.27	**−0.41**	−0.03	**0.44**
Summer	−0.06	−0.27	0.01	0.16	−0.07	−0.32
Autumn	−0.32	**−0.40**	−0.16	−0.01	−0.27	−0.34
CB						
Winter	**0.44**	0.18	−0.05	−0.29	**0.47**	0.41
Spring	**0.37**	**0.58**	−0.03	−0.09	**0.41**	**0.69**
Summer	0.18	**−0.51**	0.22	0.25	0.07	**−0.61**
Autumn	0.32	**0.49**	−0.12	−0.04	**0.39**	**0.60**
CU						
Winter	0.21	0.32	−0.02	0.04	**0.41**	**0.68**
Spring	0.34	**0.61**	0.09	**0.36**	**0.49**	**0.78**
Summer	−0.07	**−0.43**	0.04	**−0.37**	−0.15	−0.26
Autumn	−0.29	−0.25	−0.33	**−0.45**	−0.06	0.21
FO						
Winter	−0.29	**−0.63**	**−0.36**	**−0.63**	−0.14	**−0.56**
Spring	−0.22	**−0.40**	**−0.63**	**−0.67**	0.06	−0.18
Summer	0.01	**−0.48**	0.10	−0.15	−0.02	**−0.53**
Autumn	**0.51**	**0.89**	0.06	0.16	**0.53**	**0.89**
HI						
Winter	**−0.57**	**−0.73**	**−0.55**	**−0.50**	**−0.51**	**−0.81**
Spring	−0.24	**−0.62**	−0.19	−0.35	−0.19	−0.15
Summer	−0.17	**−0.50**	0.20	0.22	−0.25	**−0.47**
Autumn	**−0.39**	−0.25	**−0.40**	**−0.50**	−0.27	−0.09
NS						
Winter	**−0.57**	**−0.70**	**−0.71**	**−0.77**	**−0.39**	**−0.56**
Spring	−0.25	**−0.52**	−0.22	**−0.37**	−0.16	**−0.40**
Summer	−0.05	**−0.79**	0.09	**−0.39**	−0.08	**−0.77**
Autumn	−0.17	−0.14	−0.31	**−0.62**	−0.06	0.31
SC						
Winter	0.16	0.32	−0.13	−0.13	0.25	0.41
Spring	**−0.37**	**−0.51**	−0.30	−0.02	−0.36	−0.55
Summer	−0.12	**−0.67**	0.04	0.05	−0.12	−0.72
Autumn	**−0.45**	**−0.76**	−0.29	**−0.83**	−0.47	−0.78
ST						
Winter	**−0.37**	**−0.70**	−0.74	−0.59	−0.07	**−0.50**
Spring	**−0.49**	**−0.79**	−0.22	−0.32	**−0.44**	**−0.81**
Summer	0.00	**−0.42**	0.01	−0.58	0.00	−0.21
Autumn	0.22	**0.42**	−0.12	−0.01	0.30	**0.44**

[a]For the period 1971–1996 for each season of winter (DJF), spring (MAM), summer (JJJA), and autumn (SON) for all of Europe, southern Europe, and northern Europe. A running average of 5 years is performed to assess their low-frequency variability. Bold values indicate significance at the 95% confidence level. Abbreviations are as follows: AC, altocumulus; AS, altostratus; CB, cumulonimbus; CU, cumulus; FO, fog; HI, high-level clouds; NS, nimbostratus; SC, stratocumulus; ST, stratus; TC, total cloud.

With sunshine duration measurements being a good proxy for the DSW [*Stanhill and Cohen*, 2005; *Makowski et al.*, 2009], our results are also in agreement with *Sanchez-Lorenzo et al.* [2008] where they found significant and positive trends in winter using sunshine duration measurements in the same regions. They also found negative trends in the southern part of Europe.

[33] The spring and summer seasons with the largest absolute DSW fluxes most strongly reflect the dimming and brightening that occurs in the annual mean time series. For 1970–1985, the summer has the strongest negative trend of −3.2% decade^{-1} and is not significant, but it agrees with the increase found in the summer cloud amount for most of Europe [*Warren et al.*, 2007]. For spring during 1970–1985 the reductions in the DSW are also evident in the time series; however, their negative trends are not as large (−2.4% decade^{-1}) and is also not significant. The smaller changes during spring are explained by the smaller positive trends in cloud cover found during this season in Europe [*Warren et al.*, 2007].

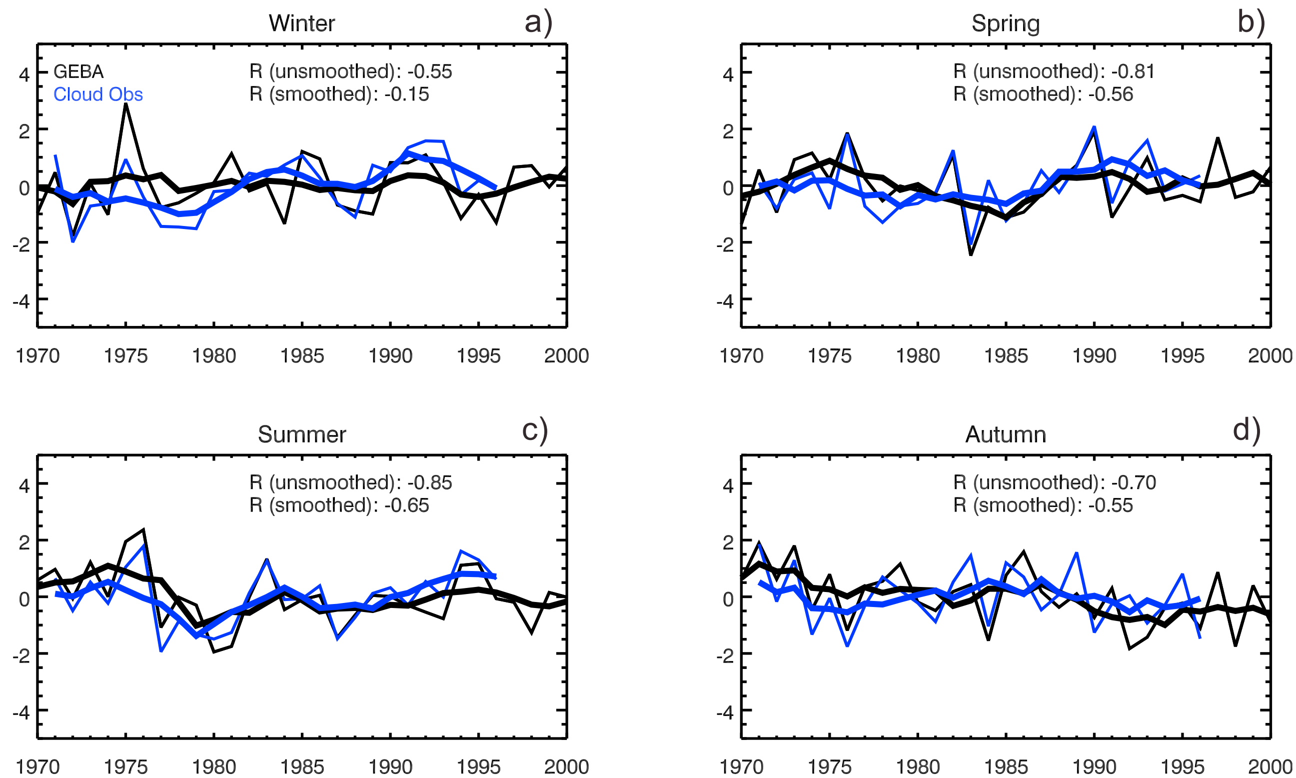

Figure 10. Seasonal mean time series: (a) winter (DJF); (b) spring (MAM); (c) summer (JJA); and (d) autumn (SON) of surface solar radiation (1970–2000) in black and the opposite of total cloud cover (1971–1996) in blue for all of Europe. The correlation coefficient computed for the period, 1971–1996, is displayed both for the unsmoothed series (high-frequency variability) and the smoothed series (low-frequency variability). The smoothed series is computed using a running average of 5 years. Units are standardized anomalies and are dimensionless.

[34] During 1985–2000 the winter reflects a clear distinct dipole pattern that develops between statistically significant positive values of DSW in the Mediterranean and negative trends that are mostly nonsignificant in the central to the northern part of Europe. This is in line with the results obtained for the correlation between the DSW and NAO index where a pattern emerged with positive values in the south and negative in the north of Europe. This can be explained by the strengthening of the positive phase of the NAO related to circulation mainly since the 1980s [*Hurrell and van Loon*, 1997; *Ulbrich and Christoph*, 1999]. In addition, a high correlation was found in southern Europe during this same period and agrees with the occurrence of the peak in the NAO index at this time [*Jones et al.*, 1997]. Also, there were increased anticyclonic circulation patterns and related decreases in cloud amounts during this season found in the southern region [*Hurrell*, 1995; *Jones et al.*, 1997; *Rodwell et al.*, 1999; *Trigo et al.*, 2002; *Warren et al.*, 2007]. The reductions in the cyclonic activity or the higher-pressure systems occurring in this region are also confirmed by *Maugeri et al.* [2001] where they found decreases in winter cloud cover in Italy and related it to the strengthening of the NAO. Other studies have also shown the influence of this circulation pattern in winter using sunshine duration measurements [*Pozo-Vázquez et al.*, 2004; *Sanchez-Lorenzo et al.*, 2008]. When the low-frequency variability of the time series is determined, the correlation between the DSW and NAO index increases suggesting a strong influence by this circulation pattern. The NAO clearly explains the distinct dipole pattern that emerges during 1985–2000 in winter.

[35] A stronger relationship was seen between cloud cover and NAO and the correlation becomes greater in the low-frequency variability. The highest correlation was found in winter in southern Europe for nimbostratus (midlevel) clouds. In general, these results agree with those found by *Warren et al.* [2007] where nimbostratus showed the strongest correlation with the North Annual Mode (NAM), which is closely related to the NAO. It is also in line with our results of the DSW and cloud cover with low-level and midlevel clouds being closely related to the DSW. These cloud types, such as stratocumulus have strong cooling effects on the Earth's surface and thus, have important implications for the sensitivity and interaction with aerosols [*Xu et al.*, 2005; *Mauger and Norris*, 2007]. Also, the strong correlation found in winter between the DSW and cloud cover decreases in the low-frequency variability, which might suggest that clouds are not the only contributing factor to the changes in DSW.

[36] In spring and summer during 1985–2000 many sites have positive DSW values that are in the range of 8–12% decade^{-1} but it is the spring from the seasonal mean time series that shows the largest absolute increase (1.6% decade^{-1}) and is not significant. The DSW and cloud cover relationship in spring and summer show the strongest

Table 5. Correlation Coefficients for Total Cloud Cover as Well as Cloud Cover From the Analysis Between Surface Solar Radiation and Cloud Cover[a]

Cloud Type	Europe	Europe (Running Average)	Southern Europe	Southern Europe (Running Average)	Northern Europe	Northern Europe (Running Average)
TC						
Winter	**−0.55**	−0.15	**−0.80**	**−0.75**	**−0.37**	0.12
Spring	**−0.81**	**−0.56**	**−0.57**	−0.27	**−0.88**	**−0.77**
Summer	**−0.85**	**−0.65**	**−0.57**	0.07	**−0.93**	**−0.81**
Autumn	**−0.70**	**−0.55**	**−0.80**	**−0.66**	**−0.63**	**−0.48**
AC						
Winter	−0.28	−0.17	**−0.37**	−0.10	**−0.36**	−0.34
Spring	**−0.58**	0.20	**−0.38**	0.08	**−0.74**	−0.31
Summer	**−0.65**	**−0.45**	**−0.42**	**0.54**	**−0.80**	**−0.78**
Autumn	**−0.56**	**−0.61**	**−0.71**	**−0.48**	**−0.47**	**−0.58**
AS						
Winter	**−0.47**	−0.35	**−0.53**	**−0.59**	−0.04	0.17
Spring	−0.34	**−0.38**	−0.29	−0.16	**−0.62**	**−0.54**
Summer	**−0.41**	−0.20	−0.03	**0.64**	**−0.54**	**−0.43**
Autumn	**−0.52**	−0.27	−0.17	**0.52**	**−0.43**	−0.28
CB						
Winter	**0.43**	**0.50**	**0.52**	0.10	0.11	0.31
Spring	0.17	**0.55**	0.27	0.13	0.01	0.33
Summer	−0.29	**−0.41**	0.16	0.02	**−0.62**	**−0.73**
Autumn	0.29	**0.74**	**0.38**	**0.73**	0.16	**0.58**
CU						
Winter	−0.04	−0.08	−0.05	−0.21	**−0.39**	**−0.57**
Spring	−0.21	−0.21	−0.43	−0.56	0.13	**0.58**
Summer	−0.31	**−0.76**	−0.19	−0.64	−0.25	**−0.48**
Autumn	**−0.65**	**−0.85**	−0.73	−0.92	−0.15	−0.19
FO						
Winter	−0.20	0.17	−0.22	−0.25	−0.03	**0.57**
Spring	**−0.38**	**−0.43**	**−0.36**	0.00	−0.36	**−0.47**
Summer	**−0.39**	−0.20	−0.04	**0.48**	**−0.48**	**−0.42**
Autumn	0.21	**0.49**	−0.10	**0.46**	−0.03	0.07
HI						
Winter	−0.08	−0.11	−0.27	−0.16	0.17	0.43
Spring	−0.36	−0.30	0.29	0.36	−0.66	−0.84
Summer	**−0.36**	**−0.53**	−0.12	**0.54**	−0.47	−0.69
Autumn	−0.33	−0.13	−0.25	0.11	−0.40	−0.49
NS						
Winter	−0.32	−0.15	**−0.87**	**−0.85**	0.10	**0.57**
Spring	**−0.70**	**−0.75**	−0.35	0.03	**−0.74**	**−0.75**
Summer	**−0.89**	**−0.78**	**−0.43**	**−0.63**	**−0.86**	**−0.73**
Autumn	**−0.50**	−0.04	**−0.78**	**−0.87**	−0.28	0.33
SC						
Winter	−0.32	−0.14	−0.32	0.03	**−0.43**	−0.80
Spring	**−0.67**	−0.16	−0.32	−0.06	**−0.61**	−0.18
Summer	**−0.84**	**−0.61**	**−0.38**	0.06	**−0.89**	**−0.72**
Autumn	**−0.77**	**−0.76**	**−0.75**	**−0.59**	**−0.59**	**−0.52**
ST						
Winter	**−0.47**	−0.20	**−0.85**	**−0.73**	−0.15	0.29
Spring	**−0.47**	**−0.42**	**−0.53**	**−0.45**	**−0.47**	**−0.38**
Summer	**−0.62**	−0.30	−0.26	**−0.57**	**−0.52**	−0.04
Autumn	−0.12	0.15	**−0.54**	**−0.72**	−0.05	0.21

[a]Bold values indicate significance at the 95% confidence level. For abbreviations, see Table 4 footnote.

correlation in all of Europe and northern Europe but decreases in the low-frequency variability. At the same time, the winter and autumn correlation is highest in southern Europe but declines as well in the lower-frequency series. Referring to all of Europe, this is in line with the work of *Stjern et al.* [2009] where lower correlations between DSW and cloud cover were reported in the autumn and winter months than during spring and summer. They attributed this weaker relation in winter and autumn to the higher concentration of aerosols during these months due to the greater stability of the atmosphere, which lower the solar radiation on clear days.

[37] The seasonal means time series for autumn continually decreased through the 1980s and 1990s, and exhibited an overall constant and significantly negative trend of −2.5% decade^{-1}. What is not apparent in this time series but can be seen in the trends of individual stations during 1985–2000 are large negative trends up to −12% decade^{-1} in southern Europe. Also, positive trends are found mostly in the central to the northern part of Europe with three sites that are significant. The overall trend pattern from these stations have the opposite dipole pattern as previously seen in winter during 1985–2000. The changes that have occurred in the NAO during autumn since about 1985 are a strengthening of

the negative phase, which explains the negative trends of the DSW in the south and positive in the north. Similar results have also been found by *Sanchez-Lorenzo et al.* [2008] with positive trends in the north and negative in the south. From our analysis of the correlation between the DSW and NAO index, a fair to good value in autumn was found during 1970–2000 and 1985–2000 in the low-frequency variability of the time series. This gives evidence that the trend detected in the DSW during autumn is largely influenced by the NAO.

[38] Overall it seems that clouds explain a great part of the high-frequency changes of the DSW in spring and summer in northern Europe and in winter and autumn in southern Europe, but have less influence in all these seasons in the low-frequency variability. The weaker relationship found between cloud cover and the DSW in the low frequency could be due to the additional influence from changes in anthropogenic aerosols, which was also the most likely explanation for the dimming and brightening given by *Norris and Wild* [2007]. At the same time because the correlation between the DSW and NAO became stronger in the low-frequency variability, primarily in winter and autumn, it suggested that an additional factor besides cloud cover is being influenced by the NAO or vice versa that in turn affects changes in DSW. This could be due to aerosols as suggested by *Gillett et al.* [2003] among a number of other forcings. Although few studies have focused on the interaction between aerosols and the NAO, it is not clear to what extent these aerosols may influence this mode of variability.

5. Conclusions

[39] The results obtained in this study of the changes in the DSW are based on a strict requirement that was set on the amount of missing data. This allows analyses to be made with a more complete time series, which include measurements made with pyranometer instruments at various stations across Europe. From these measurements, the variability of the DSW was obtained over 1970–2000 on an annual and seasonal temporal resolution but with a focus on the latter.

[40] The results from the annual time series follow the dimming and more recent brightening as is found in many other studies. From the seasonal series it is the spring and summer that show similar behavior and has been found to be correlated with clouds but only in the high-frequency variability. In the winter time series a slight increase throughout the whole period was found; however, it is not significant. Individual trends for some of the stations during this season of the first period (1970–1985) revealed statistically significant increases of DSW in central parts of Europe and mostly nonsignificant decreases in the south. The opposite pattern in winter was seen during 1985–2000, which revealed a few sites with significant increases in the Mediterranean region and nonsignificant decreases in central and northern Europe. This dipole pattern was also seen in the correlation between the DSW and NAO index for each site analyzed with positive values in the south and negative in the north. Moreover, a strong relationship was found between the DSW and NAO index in winter even in the low-frequency variability. This dipole pattern found between DSW and the NAO is consistent with other studies [*Pozo-Vázquez et al.*, 2004] and is also consistent with the dipole pattern found between the NAO and precipitation over the European region [*Hurrell*, 1995]. In autumn during 1985–2000 negative trends were found in the Mediterranean while positive trends were found in the north. We pointed out that these seasonal changes, especially in winter and autumn, are primarily due to the NAO circulation.

[41] We found that long-term changes in the DSW are highly dependent on the NAO circulation, primarily in winter and autumn in southern Europe, through cloud cover variability associated with the NAO. Even though cloud cover does explain the high-frequency DSW changes mainly in winter and autumn in southern Europe and in spring and summer in northern Europe, their correlation weakens in the lower-frequency evaluation. This suggests another influence may be acting on the decadal seasonal DSW changes, such as aerosols, which are also found in other studies to be the main cause for the annual mean decadal changes. In addition, low-level to midlevel clouds show strongest correlation with the DSW. This implies that these types of clouds are the most important in their interaction with the DSW as well as with aerosols. Also, we propose that aerosols may be an underlying influence acting on the NAO or vice versa to explain the weakening relationship of the DSW and cloud cover and the strengthening of the DSW and NAO in winter and autumn in the low-frequency variability. These changes suggest that there is another influence interfering with this relationship, which may be due to aerosols. However, further research would be needed to know for certain and to what extent they are attributable to the NAO and ultimately to the long-term changes in DSW. In a future study we plan to determine the seasonal mean trends of the solar radiation in the clear-sky and to quantify the induced effects from the seasonal mean aerosol optical depth as well as correlating these aerosols with the NAO and DSW. This will enable a further understanding of the interactions between cloud cover, induced here mainly from atmospheric circulation patterns, and aerosols and their influence on solar radiation.

[42] **Acknowledgments.** The authors would like to express their gratitude to Christoph Schaer and Atsumu Ohmura for their support. We thank Tracy Ewen, Doris Folini, and the anonymous reviewers for their helpful comments and suggestions to improve the manuscript. We thank Guido Muller, Barbara Trussel, and Knut Makowski for their support of the GEBA database. We would also like to thank Stephen Warren and Ryan Eastman for providing additional information on cloud variability from the Extended Edited Cloud Reports Archive (EECRA) and for providing cloud data from their digital database at the Carbon Dioxide Information Analysis Center (CDIAD). The NAO indices are taken from the Climate and Global Dynamics (CGD) Climate Analysis Section from NCAR (http://www.cgd.ucar.edu/cas/jhurrell/indices.html). This research is financially supported by the National Centre of Competence in Climate Research (NCCR Climate) sponsored by the Swiss National Science Foundation.

References

Abakumova, G. M., E. M. Feigelson, V. Russak, and V. V. Stadnik (1996), Evaluation of long-term changes in radiation, cloudiness, and surface temperature on the territory of the former Soviet Union, *J. Clim.*, *9*, 1319–1327, doi:10.1175/1520-0442(1996)009<1319:EOLTCI>2.0.CO;2.

Alpert, P., P. Kishcha, Y. J. Kaufman, and R. Schwarzbard (2005), Global dimming or local dimming?: Effect of urbanization on sunlight availability, *Geophys. Res. Lett.*, *32*, L17802, doi:10.1029/2005GL023320.

Ångström, A. (1962), Atmospheric turbidity, global illumination and planetary albedo of the Earth, *Tellus*, *14*, 435–454.

Behrens, K. (2007), Basic measurements of radiation at station Lindenberg (1995–02), doi: 10.1594/PANGAEA.671028, Richard Aßmann Observ., Meteorol. Observ. Lindenberg, Lindenberg, Germany.

Chiacchio, M., P. W. Stackhouse Jr., S. J. Cox, S. K. Gupta, and J. C. Mikovitz (2004), Evaluating surface measured vs. satellite-retrieved long-term surface SW fluxes by surface climatological type, *Eos Trans. AGU*, Jt. Assem. Suppl., Abstract A21A-07.

Dutton, E. G., A. Farhadi, R. S. Stone, C. N. Long, and D. W. Nelson (2004), Long-term variations in the occurrence and effective solar transmission of clouds determined from surface-based total irradiance observations, *J. Geophys. Res.*, *109*, D03204, doi:10.1029/2003JD003568.

Dutton, E. G., D. W. Nelson, R. S. Stone, D. Longenecker, G. Carbaugh, J. M. Harris, and J. Wendell (2006), Decadal variations in surface solar irradiance as observed in a globally remote network, *J. Geophys. Res.*, *111*, D19101, doi:10.1029/2005JD006901.

Gilgen, H., and A. Ohmura (1999), The global energy balance archive, *Bull. Am. Meteorol. Soc.*, *80*(5), 831–850, doi:10.1175/1520-0477(1999)080<0831:TGEBA>2.0.CO;2.

Gilgen, H., M. Wild, and A. Ohmura (1998), Means and trends of shortwave irradiance at the surface estimated from Global Energy Balance Archive data, *J. Clim.*, *11*, 2042–2061.

Gilgen, H., A. Roesch, M. Wild, and A. Ohmura (2009), Decadal changes in shortwave irradiance at the surface estimated from Global Balance Energy Archive data, *J. Geophys. Res.*, *114*, D00D08, doi:10.1029/2008JD011383.

Gillett, N. P., H. F. Graf, and T. J. Osborn (2003), Climate change and the NAO, in *The North Atlantic Oscillation: Climatic Significant and Environmental Impact*, *Geophys. Monogr. Ser.*, vol. 134, edited by J. Hurrell et al., chap. 9, pp. 193–209, AGU, Washington, D. C.

Hurrell, J. W. (1995), Decadal trends in North Atlantic Oscillation and relationship to regional temperature and precipitation, *Science*, *269*, 676–679, doi:10.1126/science.269.5224.676.

Hurrell, J. W., and H. van Loon (1997), Decadal variations in climate associated with the North Atlantic Oscillation, *Clim. Change*, *36*, 301–326, doi:10.1023/A:1005314315270.

Hurrell, J. W., Y. Kushnir, M. Visbeck, and G. Ottersen (2003), An overview of the North Atlantic Oscillation, in *The North Atlantic Oscillation: Climate Significance and Environmental Impact*, *Geophys. Monogr. Ser.*, vol. 134, edited by J. W. Hurrell et al., pp. 1–35, AGU, Washington, D. C.

Jones, P. D., T. Jonsson, and D. Wheeler (1997), Extension to the North Atlantic Oscillation using early instrumental pressure observations from Gibraltar and south-west Iceland, *Int. J. Climatol.*, *17*, 1433–1450, doi:10.1002/(SICI)1097-0088(19971115)17:13<1433::AID-JOC203>3.0.CO;2-P.

Liepert, B. G. (2002), Observed reductions of surface solar radiation at sites in the United States and worldwide from 1961 to 1990, *Geophys. Res. Lett.*, *29*(10), 1421, doi:10.1029/2002GL014910.

Liepert, B. G., and G. J. Kukla (1997), Decline in solar radiation with Increased horizontal visibility in Germany between 1964 and 1990, *J. Clim.*, *10*, 2391–2401, doi:10.1175/1520-0442(1997)010<2391:DIGSRW>2.0.CO;2.

Liepert, B. G., and I. Tegen (2002), Multidecadal solar radiation trends in the United States and Germany and direct tropospheric aerosol forcing, *J. Geophys. Res.*, *107*(D12), 4153, doi:10.1029/2001JD000760.

Lohmann, U., and J. Feichter (2005), Global indirect aerosol effects: A review, *Atmos. Chem. Phys.*, *5*, 715–737.

Long, C. N., E. G. Dutton, J. A. Augustine, W. Wiscombe, M. Wild, S. A. McFarlane, and C. J. Flynn (2009), Significant decadal brightening of downwelling shortwave in the continental United States, *J. Geophys. Res.*, *114*, D00D06, doi:10.1029/2008JD011263.

Makowski, K., E. Jager, M. Chiacchio, M. Wild, T. Ewen, and A. Ohmura (2009), On the relationship between diurnal temperature range and surface solar radiation in Europe, *J. Geophys. Res.*, *114*, D00D07, doi:10.1029/2008JD011104.

Marmer, E., B. Langmann, and H. Fagerli (2007), Direct shortwave radiative forcing of sulfate aerosol over Europe from 1900 to 2000, *J. Geophys. Res.*, *112*, D23S17, doi:10.1029/2006JD008037.

Mauger, G. S., and J. R. Norris (2007), Stratocumulus sensitivity to aerosols and dynamics, *Eos Trans. AGU*, *88*, Fall Meet. Suppl., Abstract A24B-01.

Maugeri, M., Z. Bagnati, and M. Brunetti (2001), Trends in Italian cloud amount, 1951–1996, *Geophys. Res. Lett.*, *28*(24), 4551–4554, doi:10.1029/2001GL013754.

Maugeri, M., M. Brunetti, F. Monti, and T. Nanni (2004), Sea-level pressure variability in the Po plain (1765–2000) from homogenized daily secular records, *Int. J. Climatol.*, *24*, 437–455, doi:10.1002/joc.991.

Mylona, S. (1996), Sulphur dioxide emissions in Europe 1880–1991 and their effect on sulphur concentrations and depositions, *Tellus, Ser. B*, *48*, 662–689.

Norris, J. R., and M. Wild (2007), Trends in aerosol radiative effects over Europe inferred from observed cloud cover, solar "dimming," and solar "brightening," *J. Geophys. Res.*, *112*, D08214, doi:10.1029/2006JD007794.

Ohmura, A. (2006), Observed long-term variations of solar irradiance at the Earth's surface, *Space Sci. Rev.*, *125*, 111–128, doi:10.1007/s11214-006-9050-9.

Ohmura, A., and H. Lang (1989), Secular variation of global radiation in Europe, in *IRS '88: Current Problems in Atmospheric Radiation*, edited by J. Lenoble and J. -F. Geleyn, pp. 298–301, A. Deepak Publ., Hampton, Va.

Ohmura, A., H. Gilgen, and M. Wild (1989), Global Energy Balance Archive (GEBA), Report 1: Introduction, *Zürcher Geogr. Schr.*, *34*, 62 pp.

Ohmura, A., H. Gilgen, and M. Wild (1997), Global Energy Balance Archive (GEBA), Report 3: The GEBA version 1995 database, *Zürcher Geogr. Schr.*, *74*, 105 pp.

Petrenz, N., M. Sommer, and F. H. Berger (2007), Long-time global radiation for central Europe derived from ISCCP Dx data, *Atmos. Chem. Phys.*, *7*, 5021–5032.

Philipona, R., B. Dürr, C. Marty, A. Ohmura, and M. Wild (2004), Radiative forcing - measured at Earth's surface - corroborate the increasing greenhouse effect, *Geophys. Res. Lett.*, *31*, L03202, doi:10.1029/2003GL018765.

Pinker, R. T., B. Zhang, and E. G. Dutton (2005), Do satellites detect trends in surface solar radiation?, *Science*, *308*, 850–854, doi:10.1126/science.1103159.

Power, H. C. (2003), Trends in solar radiation over Germany and an assessment of the role of aerosols and sunshine duration, *Theor. Appl. Climatol.*, *76*, 47–63, doi:10.1007/s00704-003-0005-8.

Pozo-Vázquez, D., J. Tovar-Pescador, S. R. Gámiz-Fortis, M. J. Esteban-Parra, and Y. Castro-Díez (2004), NAO and solar radiation variability in the European North Atlantic region, *Geophys. Res. Lett.*, *31*, L05201, doi:10.1029/2003GL018502.

Rodwell, M. J., D. P. Powell, and C. K. Folland (1999), Oceanic forcing of the wintertime North Atlantic Oscillation and European climate, *Nature*, *398*, 320–323, doi:10.1038/18648.

Romanou, A., B. Liepert, G. A. Schmidt, W. B. Rossow, R. A. Ruedy, and Y. Zhang (2007), 20th century changes in surface solar irradiance in simulations and observations, *Geophys. Res. Lett.*, *34*, L05713, doi:10.1029/2006GL028356.

Ruckstuhl, C., et al. (2008), Aerosol and cloud effects on solar brightening and the recent rapid warming, *Geophys. Res. Lett.*, *35*, L12708, doi:10.1029/2008GL034228.

Russak, V. (1990), Trends of solar radiation, cloudiness and atmospheric transparency during recent decades in Estonia, *Tellus, Ser. B*, *42*, 206–210.

Sanchez-Lorenzo, A., J. Calbo, and J. Martin-Vide (2008), Spatial and temporal trends in sunshine duration over western Europe (1938–2004), *J. Clim.*, *21*(22), 6089–6098, doi:10.1175/2008JCLI2442.1.

Schulz, C., et al. (2006), Radiative forcing by aerosols as derived from the AeroCom present-day and pre-industrial simulations, *Atmos. Chem. Phys.*, *6*, 5225–5246.

Stackhouse, P. W., Jr., S. K. Gupta, S. J. Cox, M. Chiacchio, and J. C. Mikovitz (2000), The WCRP/GEWEX Surface Radiation Budget Project Release 2: An assessment of surface fluxes at 1 degree resolution, paper presented at International Radiation Symposium 2000, St. Petersburg, Russia, 24–29 July.

Stanhill, G., and S. Cohen (2001), Global dimming: A review of the evidence for a widespread and significant reduction in global radiation with a discussion of its probable causes and possible agricultural consequences, *Agric. For. Meteorol.*, *107*, 255–278, doi:10.1016/S0168-1923(00)00241-0.

Stanhill, G., and S. Cohen (2005), Solar radiation changes in the United States during the twentieth century: Evidence from sunshine duration measurements, *J. Clim.*, *18*, 1503–1512, doi:10.1175/JCLI3354.1.

Stanhill, G., and J. D. Kalma (1995), Solar dimming and urban heating at Hong Kong, *Int. J. Climatol.*, *15*, 933–941, doi:10.1002/joc.3370150807.

Stjern, C. W., J. E. Kristjansson, and A. W. Hansen (2009), Global dimming and global brightening: An analysis of surface radiation and cloud cover data in northern Europe, *Int. J. Climatol.*, *29*, 643–653, doi:10.1002/joc.1735.

Streets, D. G., Y. Wu, and M. Chin (2006), Two-decadal aerosol trends as a likely explanation of the global dimming/brightening transition, *Geophys. Res. Lett.*, *33*, L15806, doi:10.1029/2006GL026471.

Tegen, I., D. Koch, A. Lacis, and M. Sato (2000), Trends in tropospheric aerosol loads and corresponding impact on direct radiative forcing between 1950 and 1990: A model study, *J. Geophys. Res.*, *105*, 26,971–26,990, doi:10.1029/2000JD900280.

Trenberth, K. E., et al. (2007), Observations: Surface and atmospheric climate change, in *Climate Change 2007: The Physical Science Basis: Working Group I Contribution to the Fourth Assessment Report of the IPCC*, edited by S. Solomon et al., pp. 237–336, Cambridge Univ. Press, New York.
Trigo, R. M., T. J. Osborn, and J. Corte-Real (2002), The North Atlantic Oscillation influence on Europe: Climate impacts and associated physical mechanisms, *Clim. Res.*, *20*, 9–17, doi:10.3354/cr020009.
Twomey, S. A., M. Piepgrass, and T. L. Wolfe (1984), An assessment of the impact of pollution on global cloud albedo, *Tellus*, *36*, 356–366.
Ulbrich, U., and M. Christoph (1999), A shift of the NAO and increasing storm track activity over Europe due to anthropogenic greenhouse gas forcing, *Clim. Dyn.*, *15*, 551–559, doi:10.1007/s003820050299.
Vestreng, V., G. Myhre, H. Fagerli, S. Reis, and L. Tarrasön (2007), Twenty-five years of continuous sulphur dioxide emission reduction in Europe, *Atmos. Chem. Phys.*, *7*, 3663–3681.
Warren, S. G., and C. J. Hahn (2002), Cloud climatology, in *Encyclopedia of Atmospheric Sciences*, pp. 476–483, Oxford Univ. Press, New York.
Warren, S. G., R. M. Eastman, and C. J. Hahn (2007), A survey of changes in cloud cover and cloud types over land from surface observations, 1971–96, *J. Clim.*, *20*, 717–738, doi:10.1175/JCLI4031.1.
Wild, M. (2009a), How well do IPCC-AR4/CMIP3 climate models simulate global dimming/brightening and twentieth-century daytime and nighttime warming?, *J. Geophys. Res.*, *114*, D00D11, doi:10.1029/2008JD011372.
Wild, M. (2009b), Global dimming and brightening: A review, *J. Geophys. Res.*, *114*, D00D16, doi:10.1029/2008JD011470.
Wild, M., A. Ohmura, and U. Cubasch (1997), GCM-simulated surface energy fluxes in climate change experiments, *J. Clim.*, *10*, 3093–3110, doi:10.1175/1520-0442(1997)010<3093:GSSEFI>2.0.CO;2.
Wild, M., H. Gilgen, A. Roesch, A. Ohmura, C. Long, E. Dutton, B. Forgan, A. Kallis, V. Russak, and A. Tsvetkov (2005), From dimming to brightening: Decadal changes in solar radiation at the Earth's surface, *Science*, *308*, 847–850, doi:10.1126/science.1103215.
Xu, K. M., T. Wong, B. A. Wielicki, and L. A. Eitzern (2005), Statistical analyses of satellite cloud object data from CERES. Part 1: Methodology and Preliminary results of the 1998 El Niño/2000 La Niño, *J. Clim.*, *18*(13), 2497–2514, doi:10.1175/JCLI3418.1.

M. Chiacchio and M. Wild, Institute for Atmospheric and Climate Science, ETH Zurich, Universitaetsstr. 16, CH-8092 Zurich, Switzerland. (marc.chiacchio@env.ethz.ch)